Revista Cubana de Meteorología

Revista Cubana de Meteorología, Vol. 28, No. 3, July-September 2022, ISSN: 2664-0880

Research Article

https://cu-id.com/2377/v28n3e07

A sensitivy study of microphysics schemes of the wrf-arw model for low-level wind shear forecast in José Martí International Airport during convective storms.

Evaluación de esquemas de microfísica del wrf-arw en el pronóstico de cizalladura del viento a bajo nivel durante tormentas convectivas en el Areropuerto Internacional José Martí.

Patricia Coll-Hidalgo[1*], Albenis Pérez-Alarcón[2,3], Pedro Manuel González-Jardines[2], Carlos Manuel Góngora-González[1], Arlett Díaz-Zurita[1]

[1]Department of Meteorology, Cuban Corporation of Air Navigation, Havana 10800, Cuba.

[2]Department of Meteorology, Higher Institute of Technologies and Applied Sciences, University of Havana, Havana 10400, Cuba

[3]Centro de Investigación Mariña, Universidade de Vigo, Environmental Physics Laboratory (EPhysLab), Campus As Lagoas s/n, Ourense, 32004, Spain.

ABSTRACT: A sensitivity study is performed with Lin, Morrison 2-moment, WSM5, and WSM6 microphysics schemes for the numerical forecast of the low-level wind shear (LLWS) derived from storms at "José Martí" International Airport using the Weather Research and Forecasting (WRF) model. As case studies, we select four storms associated with synoptic patterns that cause dangerous conditions at this aerodrome. The simulations are made for several atmosphere low levels. The influence of obstacles of comparable height with the atmospheric low-levels was taken into account to obtain the wind fields with mass consistent correction. In this paper, the evaluation process of surface variables is focus on temperature, surface pressure, relative humidity, and precipitation. The schemes did not show bigger differences among themselves. From all of the variables, relative humidity exhibits the worst results. The best performance for precipitation forecast was obtained with WSM5 in rainy season (May-October) and Lin in dry season (November-April). For LLWS sensitivity, results indicate that each hydrometeor particle concentration predicted by tested microphysics has an influence on vertical wind profiles, particularly, for low-levels. WSM5 and Lin seems the best options for microphysics scheme, although that is not conclusive.

Keywords: microphysics, WRF-ARW, low-level wind shear, convective storm.

RESUMEN: Se realizó un estudio de sensibilidad para los esquemas de microfísica de Lin, Morrison 2- moment, WSM5 y WSM6 utilizando el modelo Weather Research and Forecasting (WRF) para el pronóstico numérico de la cizalladura del viento en niveles bajos (LLWS) vinculado a tormentas convectivas en Aeropuerto Internacional "José Martí". Como casos de estudio, se seleccionan cuatro tormentas convectivas asociadas con diferentes patrones sinópticos y, por lo tanto, diferentes mecanismos de formación. Además, se aplicó el modelo de masa consistente para reducir la influencia de los obstáculos en la pista durante la interpolación del campo de viento. Se desarrolló inicialmente una evaluación de la configuración del modelo, para las variables en superficie: temperatura, presión atmosférica, humedad relativa y precipitación. Los esquemas no mostraron diferencias significativas, pero la humedad relativa presentó los peores resultados. El mejor desempeño para el pronóstico de precipitación se obtuvo con WSM5 en el periodo lluvioso (mayo-octubre) y Lin en el poco lluvioso (noviembre-abril). Los resultados revelan que la concentración de partículas de cada tipo de hidrometeoro resuelto por las microfísicas en estudio, repercute en los perfiles verticales de viento durante las tormentas. En general, WSM5 y Lin resultaron los esquemas de microfísica más hábiles en el modelo WRF para predecir la cizalladura del viento en niveles bajos en la región de estudio, pero se requieren más estudios para generalizar nuestros hallazgos.

Palabras claves: esquema de microfísica, WRF-ARW, cizalladura del viento en niveles bajos, tormenta convectiva.

*Correspondence to: Patricia Coll-Hidalgo. E-mail: patricia.coll@aeronav.avianet.cu

Received: 24/08/2021

Accepted: 27/07/2022

1. INTRODUCTION

The wind field forecast is one of the most important meteorological supports for air operations. Wind shear is always present in the atmosphere; their significance to aviation lies in its effect on aircraft performance. Low-level wind shear (LLWS), in the broadest sense, encompasses a family of air motions in the lower level of the atmosphere, ranging from small-scale eddies and gustiness that may affect aircraft as turbulence. (OACI, 2005)

Some equipment can be used to provide alert service (Wilson *et al.*, 2005; Campbell & Olson, 1987; Hermes, Witt & Smith, 2008). Most recently, laser detection and ranging have been used to detect the LLWS (Shun & Chan, 2008; Chan & Lee, 2011; Jiang *et al.*, 2012). Numerical Weather Prediction (NWP) models are an alternative to be used as LLWS alarm systems in aeronautics (Boilley & Mahouf, 2008; Shaw *et al.*, 2008; Urlea & Pietrisi, 2015; Hon, 2020).

Boilley *et al.* (2008) developed a preliminary investigation towards mesoscale data assimilation at high resolution (between 500 m and 2.5 km) for the detection and prediction of boundary layer weather hazards for air traffic. The authors verified the capacity of the numerical model Meso-NH to simulate horizontal wind shear near Nice airport. On the other hand, Shaw *et al.* (2008) implemented the Weather Research and Forecasting (WRF) model with the dynamical core Advanced Research WRF (ARW) v2.2 model (Skamarock *et al.*, 2005) for the Dubai International Airport´s aviation weather decision support system. The authors installed an operational system assimilating satellites data, radiometers, wind profiles, radar, and surface observations. In the Hong Kong International Airport, a subkilometric NWP capability in capturing LLWS was evaluated (Hon, 2020). This Aviation Model (AVM) (Chan & Hon, 2016; Hon, 2018) is a subkilometer resolution implementation of the WRF.

The WRF model, like most of NWPs, offers several physics options. For wind forecast, commonly, sensitivity boundary-layer parametrizations (PBL) studies were developed (Srinivas, Venkatesan and Bagavath Singh, 2007; Miao *et al.*, 2009; Storm & Basu, 2010; Hu, Nielsen-Gammon & Zhang, 2010; Carvalho *et al.*, 2012; Hu, Klein & Xue, 2013; Garcia-Diez *et al.*, 2013; Srikanth *et al.*, 2014; Boadh & Satyanarayana, 2014). In Cuba, the meteorological model WRF-ARW sensitivity to physics options was tested (Sierra *et al.*, 2017; Sánchez, 2018). The Immediately Prediction System (SiSPI, spanish acronym) (Sierra *et al.*, 2015) and the Numerical Prediction System Ocean-Atmosphere (SPNOA, spanish acronym) (Pérez-Bello *et al.*, 2019) were developed and implemented in the Center of Atmospheric Physics of the Institute of Meteorology of Cuba (INSMET, spanish acronym), but not specific to the aviation application.

For this purpose, Coll-Hidalgo *et al.* (2021) improve a preliminary evaluation of numerical surface wind field forecast with WRF-ARW model over "José Martí" International Airport. In the study area Coll-Hidalgo *et al.* (2021) pointed out that in both rainy and dry seasons, was observed pronounced differences in errors for wind speed and direction. Furthermore, in this airport located in a complex orography near the elevations of Cacahual, the primary source of LLWS and dangerous wind hazards providing for storms in the aerodrome vicinity (Sosa, 2018). Skills metrics indicated a more accurate forecast in dry season storms than in the rainy season ones, a source of errors is possibly the fact that the storms were produced from different conditions. Microphysics parametrizations are significant in predicting storms (Rajeevan *et al.*, 2010; Han, Baik & Khain, 2012; Hadler *et al.*, 2015; Shrestha *et al.*, 2017). Also, convective storms develop are sensitive to the microphysics schemes (Sari, Baskoro & Hakim, 2018; Reisner, Rasmussen & Bruintjes, 1998; Liu & Moncrieff, 2007; Otkin & Greenwald, 2007; Liu *et al.*, 2011; Rajeevan *et al.* 2010). Coll-Hidalgo *et al.* (2021) remarks that the position and size of simulated storms, and, those features modified the surface wind field were changed because of tested microphysics.

Updrafts and downdrafts relative to storms generate variations in the three dimensions of the wind field. The aircraft is especially susceptible to the adverse effects of low-level wind shear, cause during the climbout and approach phases of flight, aircraft airspeed and height is near critical values. In this study, we aim to develop a microphysics sensitivity study pre-, in-, and, after- storms, to provide the best WRF-ARW model configuration for the forecasting of LLWS derived from storms in "José Martí" International Airport.

2. OBSERVATIONAL AND MODELLED DATA

2.1 WRF-ARW and RAP model

The WRF v.3.9 model (Skamarock *et al.*, 2008) was used with ARW dynamic core. The simulations comprised a 12/4 km two-way nested domains (Figure 1) and 34 verticals levels. Briefly, the setup includes for both domains (Coll-Hidalgo *et al.*, 2021): Rapid Radiative Transfer Model longwave radiation parametrization (Mlawer *et al.*, 1997), Dudhia shortwave radiation scheme (Dudhia, 1989), Unified Noah land-surface model (Tewari *et al.*, 2004), Grell-Freitas Ensemble cumulus parametrization (Grell & Freitas, 2013), Mellor-Yamada-Janjic planetary boundary layer (Janjić, 2001). The model was initialized and forced at the boundaries, with every three hourly updates, by 0.500 Global Forecast System (GFS) forecast outputs, which are freely available at https://nomads.ncep.noaa.gov/cgi-bin/filter_gfs_0p50.pl.

Storms simulations were performed with four selected microphysics schemes: Lin (Lin *et al.*, 1983), Morrison 2-moment (Morrison, Thompson & Tatarskii, 2009), WSM5 (Hong *et al.*, 2004), and WSM6 (Hong & Lim, 2006). Table 1 shows the main species of prognostic variables in these schemes. The selection was based on their use and performance in numerical weather forecast systems operating in Cuba (Sierra *et al.*, 2015; Pérez-Bello *et al.*, 2019). The forecasts were for 54 hours, started from the storm observation date at 0000 UTC.

To verify the accuracy of the LLWS forecast was used the Rapid Refresh model (RAP) analysis (Benjamin *et al.*, 2016) (https://www.ncdc.noaa.gov/data-access/model-data/model-datasets/rapid-refresh-rap). In the RAP analysis, the horizontal wind components are updated variables in Gridpoint Statical Interpolation analysis system (GSI)/RAP assimilation. According to Benjamin *et al.* (2016), the analysis method used for those variables is GSI hybrid ensemble-variational analysis. For wind components, the use of GSI permits assimilation of NOAA 405 MHz profiler wind data (decommissioned 2014), boundary layer (915 MHz) profiler wind data, radar data, aircraft data, surface/METAR-land, surface/mesonet-land, bouy/ship and GOES atmospheric motion vectors. Although the study area was near the boundaries of the RAP domain, the RAP analysis data was used as preliminary source for evaluation.

2.2 Observational data

The study area was "José Martí" International Airport (Figure 2a). It was selected because it constitutes the airport with the highest number of air operations in Cuba. Furthermore, the airport is surrounded by terrain with complex orography. "José Martí" International Airport is located in the inland forecast region of the Artemisa, Havana, and Mayabeque provinces (Figure 2b).

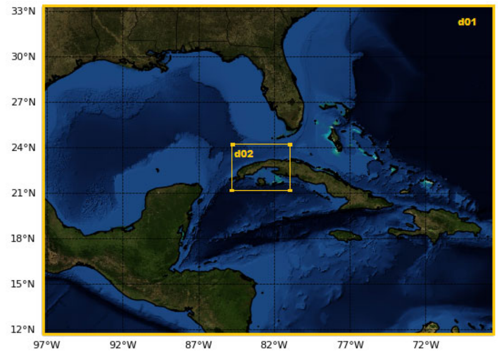

Figure 1. Simulations domains.

Sosa (2018) describes the behaviour of the LLWS over "José Martí" International Airport. LLWS is associated with meteorological systems: cold front (18.36 %), anticyclone (53.06 %), and tropical wave (10.20 %) (Sosa, 2018). The author identified the following synoptic patterns as the most frequent in which low-level wind shear occurs:

i. Influence of the North Atlantic Subtropical Anticyclone with trough medium and high levels.

ii. Influence of the North Atlantic Subtropical Anticyclone in the entire tropospheric column.

Table 1. Details of the microphysics schemes considered in the study. (Y: yes, N: no) (Skamarock *et al.*, 2008)

Microphysics schemes	Number of Moisture variables	Ice-Phase Processes	Mixed-Phase Processes
Lin	6	Y	Y
Morrison 2-moment	10	Y	Y
WSM5	5	Y	N
WSM6	6	Y	Y

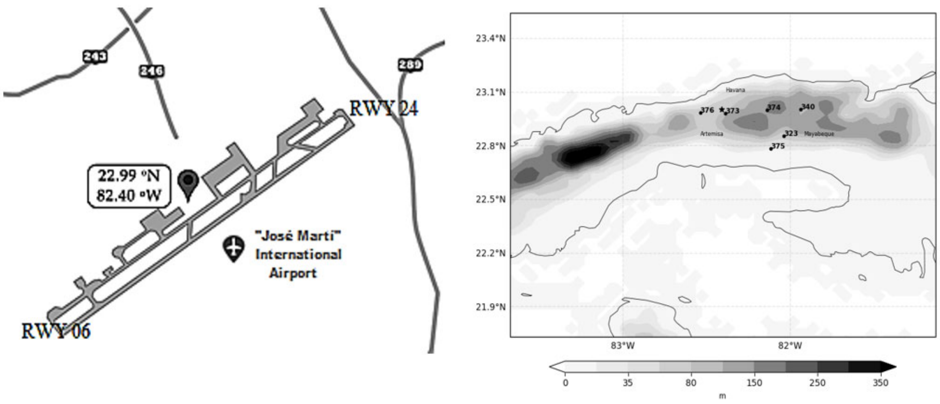

(a) (b)

Figure 2. Study area (a) "José Martí" International Airport runway (b) Artemisa-Havana-Mayabeque provinces topography (shaded) and meteorological observational stations (markers).

iii. Migratory anticyclones.

iv. Tropical waves into the south of western Cuba.

v. Cold fronts on western Cuba.

Sosa (2018) refers to that significant wind field variations over the airport are often reported under storms. As case studies, four storms associated with synoptic patterns that cause dangerous conditions at this aerodrome were selected, as shown in Table 2.

Meteorological data from the weather station in the "José Martí" International Airport was used to evaluate the surface forecast. The storms were frequently placed in the aerodrome vicinity (Figure 3). In addition, to better capture details of simulations were utilized observations from weather stations placed in the inland forecast region of the Artemisa, Havana, and Mayabeque provinces (Figure 2b).

3. METHODOLOGY

3.1 Post-processing WRF-ARW output files

In this paper, it was used the WRF-ARW output variables T2 (temperature at 2 m, K), PSFC (surface pressure, Pa), Q2 (vapor mixing ratio at 2 m, kg/kg), U (x-wind component, m/s), V (y-wind component, m/s), U10 (x-wind component at 10 m, m/s), V10 (y-wind component at 10 m, m/s), RAINC (accumulated total cumulus precipitation, mm), Air Force Weather Agency (AFWA)_LLWS (AFWA_diagnitics (Creighton *et al.*, 2014): 0-2000 ft wind shear, m/s). Relative humidity was determined using Clausius-Clapeyron (Iribarne & Godson, 1981) as follow:

$$RH = 0.263pq\left[exp\frac{17.67(T-T_0)}{T-29.65}\right]^{-1} \quad (1)$$

Where:

T= temperature (K)

p= pressure (Pa)

q= specific humidity or the mass mixing ratio of water vapor to total air (dimensionless)

T_0= reference temperature (typically 273.16 K)

3.2 Calculation of LLWS

LLWS was determined by calculation for components (OACI, 2015), as a difference between wind vectors from one point in space to another. LLWS is defined as a vector difference from surface to 500 m (Boilley & Mahouf, 2008; Díaz-Zurita *et al.*, 2021) or 600 m (OACI, 2015; Urlea & Pietrisi, 2015; Iribarne & Godson, 1981). In this paper, the forecast includes LLWS speed and direction, in sub-layers from 0-600 m (Figure 4a). These layers make it possible to detect and forecast wind shear caused by smaller-scale

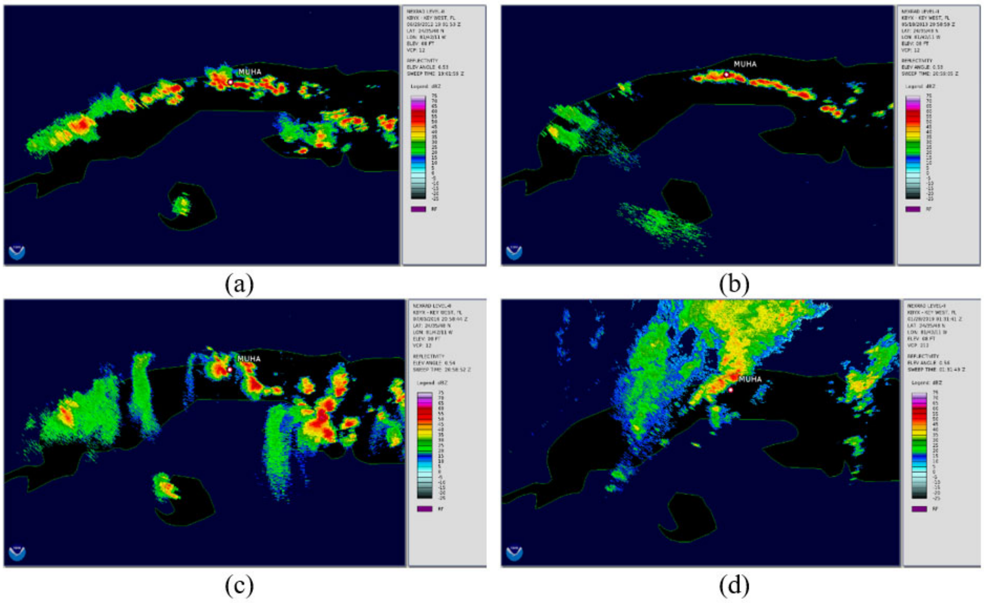

Figure 3. Key West radar reflectivity image (a) June 29th, 2012 at 19:01 UTC (b) May 18th, 2013 at 20:58 UTC (c) July 3rd, 2016 at 20:58 UTC (d) January 28th, 2019 at 01:31 UTC.

Table 2. Storms case studies (Synoptic patterns as the numbered list)

Date	Time[1]	Synoptic patterns
2012-06-29	19:01	i
2013-05-18	21:03	iii
2016-07-03	20:58	iv
2019-01-27	25:31	v

[1]Forecast hours started from the storm observation date at 0000 UTC.

storms. Furthermore, the sub-layers LLWS forecast is necessary to support meteorological service. The forecast accuracy, in this case, strongly dependent on the scale on which the wind shear operates relative to the size of the aircraft.

The density of the nodes in the neighborhood of the airport in the domain of 4 km (d02) of the resolution is low. For this reason, the rectangular grid developed by Díaz-Zurita *et al.* (2021) was used for wind field simulation. This grid takes into account the orientation (60^0 from the north) and the length of the runway (4 km). Five points are matched: one in the center of the runway (MID), one at each headland, and the other two points at 1 km from the center. The grid with a longitudinal resolution of 0.87 km and a latitudinal resolution of 0.5 km is shown in Figure 4b.

Based on Díaz-Zurita *et al.* (2021) results, for wind interpolation, we use the natural neighbor method. In addition, following Díaz-Zurita *et al.* (2021) recommendations, a correction to the interpolated WRF-ARW wind field is applied with a consistent mass model.

This model is based on the equation of continuity for an incompressible air mass moving in a two-dimensional domain, Ω, with a velocity field $\vec{u}(u,v,w)$:

$$\frac{\partial p}{\partial t} + \vec{\nabla}\cdot\left(\rho\vec{u}\right) = 0 \quad (2)$$

If the constant air density is considered for the entire domain, the equation becomes:

$$\vec{\nabla}\cdot\vec{u} = 0 \quad in \ \ \Omega \quad (3)$$

Which joins the impenetrability condition on the ground Γ_b , thus constituting the boundary condition:

$$\vec{\eta}\cdot\vec{u} = 0 \quad in \ \Gamma_b \quad (4)$$

From conditions (3) and (4), the consistent mass models pose a least-squares problem with the velocities to adjust $\vec{u}(u,v,w)$ from the observed $\vec{u}_0(u_0,v_0,w_0)$ in the Ω domain, according to the functional:

$$E(u,v,w) = \iiint\left[\alpha_1{}^2(u-u_0)^2 + \alpha_2{}^2(v-v_0)^2\right] \left(+\alpha_3{}^2(w-w_0)^2\right)dxdydz \quad (5)$$

where { $u(x,y,z)$, $v(x,y,z)$, and $w(x,y,z)$, } are the wind components calculated by the model through fit; {$u_0(x,y,z)$, $v_0(x,y,z)$, and $w_0(x,y,z)$, } are the components of the initial field, interpolated from the observations, and $\alpha_1, \alpha_2, \alpha_3$ are the Gaussian precision modules (Montero *et al.*, 2006). Considering α_1 and α_2 identical, for horizontal directions the functional to minimize (5) is:

$$E(u,v,w) = \iiint\left[\alpha_1{}^2(u-u_0)^2 + (v-v_0)^2\right] \left(+\alpha_2{}^2(w-w_0)^2\right)dxdydz \quad (6)$$

The search field $\vec{v}(u,v,w)$ will be the solution to the problem:

Find $\vec{v} \in$ K such that,

$$E\left(\vec{v}\right) = \min_{\vec{u}\in K} E\left(\vec{u}\right), K = \left\{\vec{u};\ \vec{\nabla}\cdot\vec{u} = 0, \vec{n}\cdot\vec{u}\Big|_{\Gamma_b}\right\} \quad (7)$$

This problem is equivalent to finding the saddle point at ($\overrightarrow{u,\Phi}$) of the Lagrangian:

$$L\left(\vec{u},\lambda\right) = E\left(\vec{u}\right) + \int \lambda\vec{\nabla}\cdot\vec{u}\,d\Omega \quad (8)$$

The technique of Lagrange multipliers allows obtaining the saddle point of the expression (9), $L\left(\vec{u},\lambda\right) \le L\left(\vec{u},\Phi\right) \le L$) such that the solution field is obtained from the Euler-Lagrange equations:

$$\vec{v} = \vec{v_0} + T\,\vec{\nabla}\vec{\Phi} \quad (9)$$

Where Φ is the Lagrange multiplier and $T = [T_h, T_h, T_v]$ is the transmission diagonal tensor:

$$T_h = \frac{1}{2\alpha_1^2} T_v = \frac{1}{2\alpha_2^2} \quad (10)$$

$$u = u_0 + T_h\frac{\partial\Phi}{\partial x}, v = v_0 + T_h\frac{\partial\Phi}{\partial y}, w = w_0 + T_v\frac{\partial\Phi}{\partial z} \quad (11)$$

If α_1 , α_2 are considered constant throughout the domain, the variational formulation leads to an elliptic

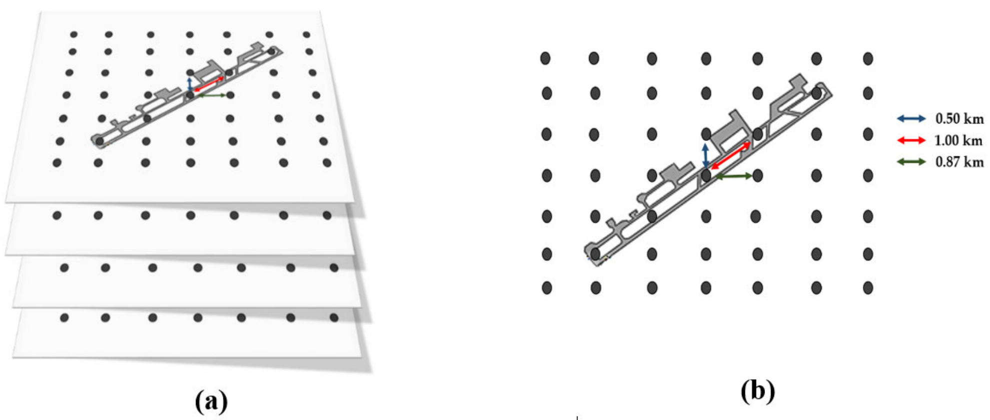

Figure 4. Rectangular grid (a) interpolation and (b) resolution.

equation defined in Φ. Indeed, substituting equation (9) in (3) results:

$$-\vec{\nabla}\cdot\left(T\,\vec{\nabla}\right)=\vec{\nabla}\cdot\vec{u_0} \quad (12)$$

Which is completed by the null Dirichlet condition at permeable boundaries (vertical domain boundaries)

$$\Phi = 0 \;\; in \;\; \Gamma_a \quad (13)$$

And Neumann's condition in the raincoats (terrain and upper border)

$$\vec{n}\cdot\vec{\nabla}\Phi = -n\cdot\vec{v_0} \;\; in \;\; \Gamma_b \quad (14)$$

Considering T_h and T_v constant, equation (12) becomes:

$$\frac{\partial\Phi^2}{\partial x^2}+\frac{\partial\Phi^2}{\partial y^2}+\frac{T_v}{T_h}\frac{\partial\Phi^2}{\partial z^2}=\frac{-1}{T_h}\left(\frac{\partial u_0}{\partial x}+\frac{\partial v_0}{\partial y}+\frac{\partial w_0}{\partial z}\right) \quad (15)$$

Eliminating the vertical component (two dimensions) was obtained:

$$\frac{\partial\Phi^2}{\partial x^2}+\frac{\partial\Phi^2}{\partial y^2}=\frac{-1}{T_h}\left(\frac{\partial u_0}{\partial x}+\frac{\partial v_0}{\partial y}\right) \quad (16)$$

This methodology guarantees the conservation of wind direction due to the impenetrability conditions.

3.2 Evaluation

In this work, for the forecast verification was calculated some statistical metrics: mean systematic error or BIAS, standard deviation (SD), root mean squared error (RMSE) and Pearson correlation coefficient. Precipitation is a dichotomous variable; therefore, it is convenient to construct a contingency table. According to Jolliffe and Stephenson (2003), some performance measures were computed. These measurements are determined from each category defined in Table 3.

$$H=\frac{a}{a+c} \quad (17)$$

The hit rate (H) is the proportion of occurrences of precipitation event that where correctly forecast.

$$F=\frac{b}{b+d} \quad (18)$$

False Alarm Rate (F), is the proportion of non-occurrences that were incorrectly forecast.

$$PC=\frac{a+d}{n}\,;n=a+b+c+d \quad (19)$$

Proportion Correct (PC) of forecast is given for equation (19).

$$FAR=\frac{b}{a+b} \quad (20)$$

False Alarm Ratio (FAR) is the proportion of forecasts of occurrences that were not followed by an actual occurrence. FAR is a sample estimate of the conditional probability of a false alarm given that occurrence was forecast.

$$CSI=\frac{a}{a+b+c} \quad (21)$$

Critical Success Index (CSI) can be regarded as a sample estimate of the conditional probability of a hit given that the event of interest was either forecast, or observed, or both. Perfect skill (H=1, F=0) gives a CSI with the maximum value of 1.

$$GSS=\frac{a-a_r}{a-a_r+b+c} \quad (22)$$

Gilbert's skill score (GSS) is a modification of CSI to allow for the number of hits that would have been obtained purely by chance. In equation (22), a_r is the number of hits expected by forecasts independent of observations (pure chance) given by:

$$a_r=\frac{(a+b)(a+c)}{n}\,;n=a+b+c+d \quad (23)$$

To obtain the best microphysics scheme to reproduce the LLWS derived from storms the analysis was developed pre-, in-, and after- the occurrence of the event Sari, Baskoro, & Hakim (2018).

4. RESULTS AND DISCUSSION

4.1 Impact of different microphysical parameterizations on surface variables

(Coll-Hidalgo *et al.*, 2021) found simulated wind surface field evaluation as a difficult criterion to consider the best microphysical scheme for wind forecast. However, the authors pointed out that WSM6 and Lin occasionally exhibit better scores. The wind at 10 meters is the lower height of LLWS calculation layers, therefore, include other sensitivity meteorological surface field analysis for determinate the best WRF-ARW configuration is a priority. In this paper, the evaluation process of surface variables is focus on temperature, surface pressure, relative humidity, and precipitation.

The schemes did not show significant differences among themselves. In previous research for a convective storm over the Nepal Himalayas (Shrestha, Connolly & Gallagher, 2017) and a hail event over Surabaya, Indonesia (Sari, Baskoro, & Hakim, 2018), the authors reported that the microphysics schemes are not sensitive to surface properties.

From all of the variables, relative humidity has the worst results. It performs poorly in hourly bias (Figure 5). The relative humidity results are not good about 1800 UTC in rainy season (Figure 5a), it is probably because a poor representation of the size and position of storms. For the dry season, about 2100 UTC, during the daily minimum relative humidity, maximum biases are showed (Figure 5b). The rainy season biases are bigger than dry season ones,

Table 3. Schematic contingency table. The numbers of observations in each category are represented by a,b,c and d. (Jolliffe and D. Stephenson, 2003)

		OBSERVATIONAL DATA	
		YES	NO
WRF-ARW	YES	HIT (a)	FALSE ALARM (b)
	NO	MISS (c)	CORRECT REJECTION (d)

this behavior strongly indicates the combination of storms relative humidity field deviations and the overestimation of the minimum daily value.

Temperature surface field biases matrix depicted the best skill, the maximum overestimation for both rainy and dry season are at 0000 UTC (Figure 6). According to the Figure 6a, under storms (approximately 2100 UTC) the temperature forecast overestimates observations. Once more, every scheme produced slightly different hourly bias.

The same slightly different microphysics performance is describing by surface pressure (Figure 7). In this case, skills are strongly dependent on the change of surface pressure due to meteorological phenomena. The dry season storm case analysed was derived from the synoptic pattern cold front. One of the main characteristics of this type of phenomenon is the falling surface pressure. A cold front crossed over the study area between 24 and 27 forecast hours. Biases for this period show large bias in the data (Figure 7b).

The Table 4 exhibits the indices that describe the correspondence between forecasts and observations of precipitations events. These values are comparable with those obtained in the evaluations developed for WRF-ARW configurations in Cuba (Sierra *et al.*, 2015; Pérez-Bello *et al.*, 2019). In this investigation, the authors verify the precipitation forecast in domains, periods, and from data that lead from the numerical experiments in this paper. However, SisPI precipitation events verification (Sierra *et al.*, 2015) have a FAR of 0.724 and a CSI of 0.113 for a 27 km domain and microphysics scheme WSM5. The same microphysics in our numerical experiments configurations have FAR results above 0.529 and lower than 0.894. CSI range from 0.113 to 0.347. The extremes CSI values correspond to the June 29, 2012 and January 27, 2019 case studies date. In a perfect skill, CSI should have a maximum value of one, and FAR be equal to zero.

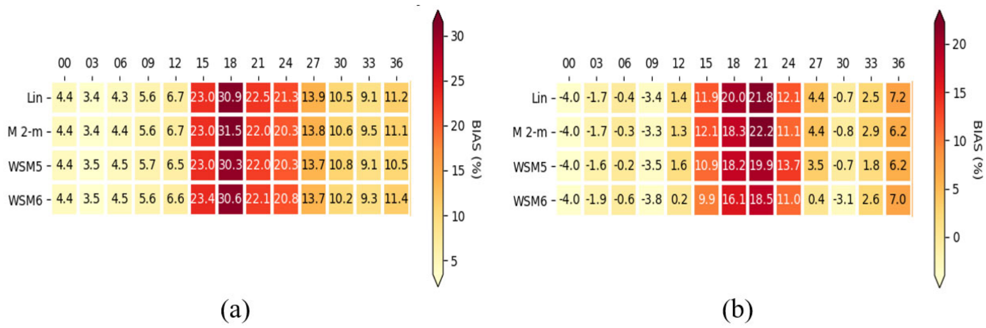

Figure 5. Matrix biases for relative humidity (a) rainy and (b) dry seasons

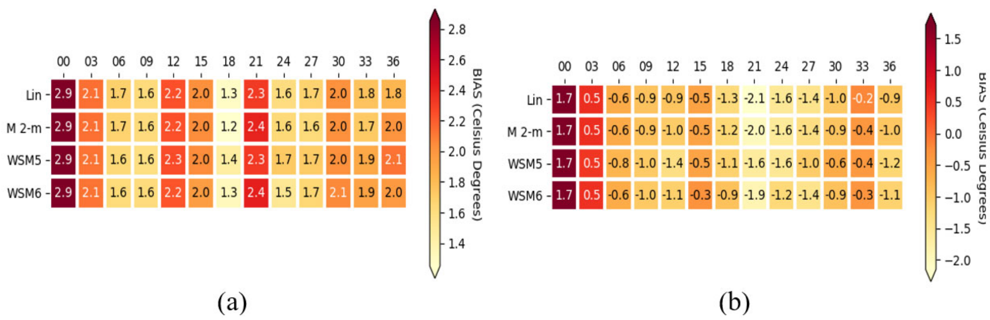

Figure 6. Matrix biases for temperature at 2 m (a) rainy and (b) dry seasons.

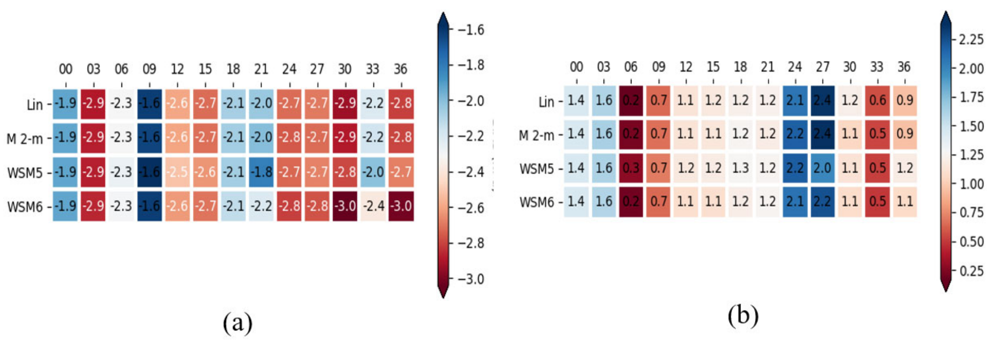

Figure 7. Matrix biases for surface pressure (a) rainy and (b) dry seasons.

The best performance for June 29, 2012 was obtained with Morrison 2-moment and Lin schemes. In the figure 8 are represented the simulated precipitation field with Morrison at 2100 UTC and the location of the surface weather stations.

Even so, the high detection of precipitation events is probably associated with the fact that Morrison is characterized by producing a wide area of stratiform precipitation associated with storms (Morrison, Thompson & Tatarskii, 2009).

During the dry season, the Lin scheme has the better results. January 27th exhibits the highest detection of events. The flux imposed by the extratropical cyclone and the LTPF influence propitiated the wide distribution of precipitation areas, which persisted temporarily.

In general, the model did well for temperature, the rest of the variables have superior biases in presence of storms. Large errors in relative humidity were also found by Somos-Valenzuela and Manquehual-Cheuque (2020) over the Northern Patagonian Icecap (NPI) and Baker River Basin. Tested schemes produced slightly different BIAS. Some remarkable differences were depicted for precipitation events verification. It is because the precipitation field should be sensitive to storm features simulation as position, size, and convection intensity.

4.1 LLWS derived from storms sensitivity

June 29th, 2012 is the storm that caused the highest wind speeds records on the runway, for this case study, we focus on the influence of convection intensity in the wind field at height.

In absence of storms, wind barbs verticals profile not show significant differences. On the other hand, microphysics schemes derived dissimilarities winds barbs verticals profiles for weak and deep convection.

Table 4. Verification measures for precipitation forecast.

Case studies	Microphysics	H	FAR	CSI	F	PC	GSS
2012-06-29	Lin	0.500	0.864	0.119	0.299	0.683	0.100
	Morrison 2-moment	0.599	0.849	0.136	0.317	0.675	0.115
	WSM5	0.500	0.871	0.113	0.317	0.666	0.096
	WSM6	0.400	0.894	0.090	0.317	0.658	0.076
2013-05-08	Lin	0.800	0.813	0.177	0.327	0.683	0.152
	Morrison 2-moment	0.699	0.829	0.159	0.317	0.683	0.135
	WSM5	0.800	0.804	0.186	0.308	0.692	0.159
	WSM6	0.699	0.815	0.170	0.289	0.709	0.145
2016-07-03	Lin	0.625	0.642	0.294	0.178	0.794	0.232
	Morrison 2-moment	0.437	0.719	0.205	0.178	0.769	0.158
	WSM5	0.375	0.760	0.171	0.188	0.752	0.130
	WSM6	0.562	0.709	0.236	0.217	0.752	0.183
2019-01-27	Lin	0.571	0.478	0.375	0.354	0.615	0.103
	Morrison 2-moment	0.500	0.511	0.328	0.354	0.586	0.085
	WSM5	0.571	0.529	0.347	0.435	0.567	0.093
	WSM6	0.547	0.520	0.343	0.403	0.576	0.091

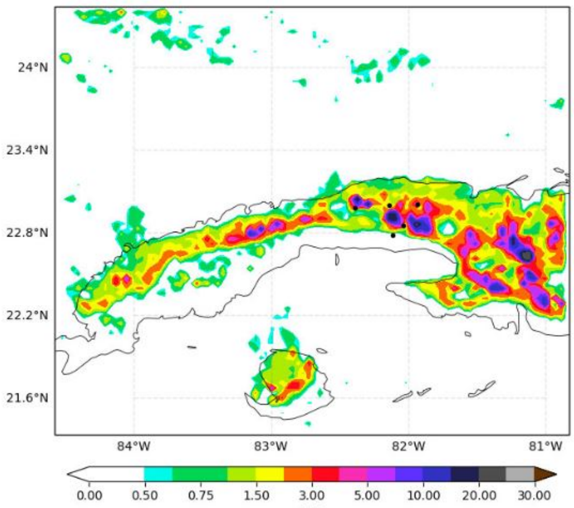

Figure 8. June 29th, 2012, simulated reflectivity with Morrison 2-moment scheme, meteorological observational stations (markers).

We dismiss the effect of the storm position, which enforces both size and intensity simulated features. The larger variations are depicted in lower levels, the same altitudes with maximum reflectivity values. For WSM5 and Lin schemes, under deep convection conditions (Figure 9a) more strong winds were simulated above 1 km. In reflectivity representation, also, WSM5 and Lin performed the maximum reflectivity cores in lower levels (Figure 9b and Figure 9d respectively). Coll-Hidalgo *et al.* (2021) pointed out perceptible variations in the profile-mixing ratio of hydrometeor particles for a storm over "José Martí" International Airport the June 29, 2012. Finally, our results indicate that each hydrometeor particle concentration predicted by tested microphysics has an influence on vertical wind profiles, particularly, for inferior heights. On behalf of our purpose, it is a substantial reason that aimed to evaluate LLWS derived from storms sensitivity of microphysics schemes.

In figure 10, we can see the Pearson correlation coefficient between the wind shear speed in the 0-2000 ft layer obtained from the AFWA-diagnostics module and the methodology applied in this investigation. It is observed how the correlation between variables is lower for the case of July 3, 2016, while for the rest of the cases the linear relationship oscillating between 0.75 and 1. The configuration with the WSM5 scheme shows the highest correlation in the cases of the rainy season, while Lin exhibits the best correlation in the case January 27, 2019.

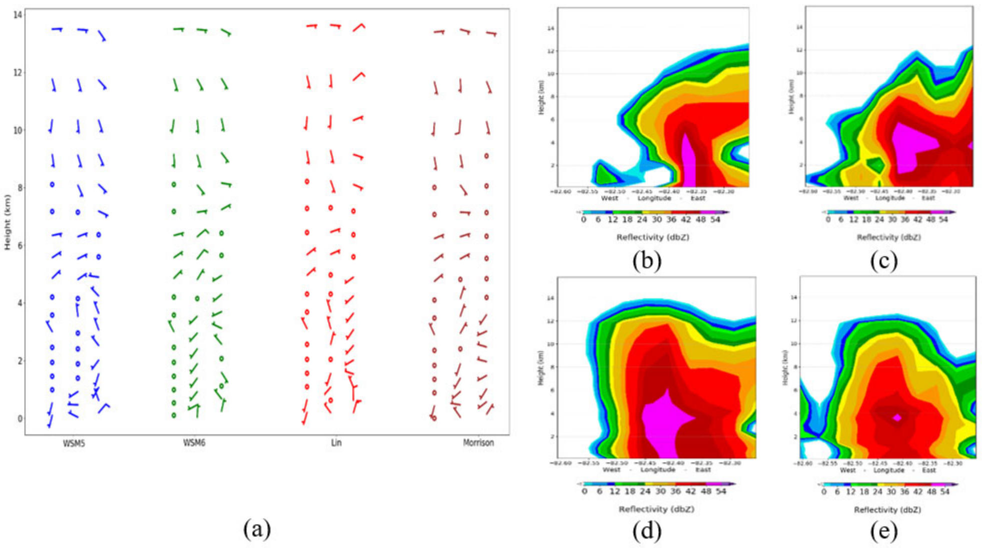

Figure 9. In (a) Wind barbs at height over airport the June 29th, 2012, from left to right of each microphysics are wind bars in absence of storms, wind barbs in presence of weak convection, and wind barbs in presence of deep convection. Deep convection reflectivity simulation with (b) WSM5, (c) WSM6, (d) Lin and (e) Morrison 2-moment schemes.

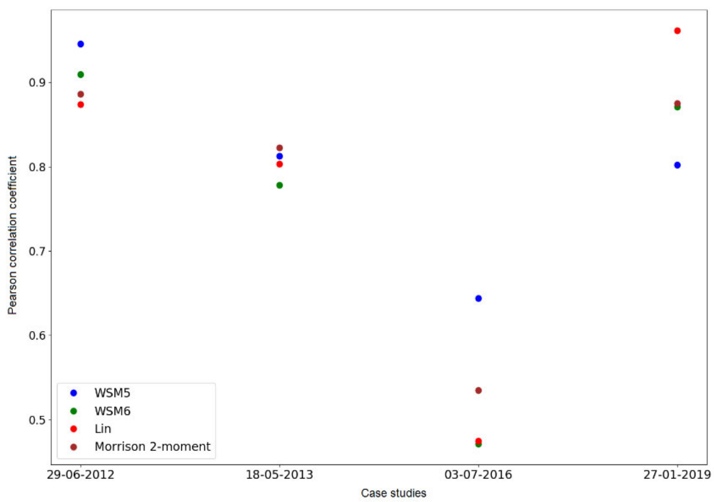

Figure 10. Pearson correlation coefficient between the wind shear speed in the 0-2000 ft layer obtained from the AFWA-diagnostics module and the methodology applied in this investigation.

Figure 11. Taylor diagrams for rainy season LLWS speed forecast, panel from left to right pre-, in-and after- storm statics at (a,b,c) 0-360 ft (d,e,f) 0-1060 ft (g,h,i) 0-1770 ft (j,k,l) 0-2500 ft.

Figure 11 shows Taylor diagrams form evaluation of LLWS speed derived from rainy season storms studies cases over "José Martí" International Airport. In WRF-ARW LLWS speed forecast verification with RAP model, all the layers of calculation have a SDs lower than 4.5 m/s, with an average maximum RMSE of 4 m/s. Pearson correlation coefficient shows negative values, schemes often depict a moderate to strong inverse correlation. Therefore, this performance may be related to use spatial resolutions. In our numerical experiments, spatial resolution is 4 km, while RAP model resolution analysis data is 13 km, which make it impossible to capture local features.

Accuracy differences between before-, in- and after-storms LLWS speed forecast are very high when compared to statics among calculation layers. In addition, for the time lapse before- occurrence of storms in the study area all microphysics have similar results, as it can been see in the Taylors diagrams (Figure 11a, d, g, h). At the same period, the highest layer shows weak positive correlation of WSM6 scheme, but whit the biggest SD and RMSE. During storms influence we can see larges variations in microphysics behavior. Microphysics performance depends on which static is considered to evaluate results. In storms lapse, Morrison 2-moment has a poorly correlation, with the lowers SD and RMSE. WSM5 and Lin schemes before- storms have SD and RMSE above 1.50 m/s, which increasing after-storms upper to 2.40 m/s. Is necessary take into account that the designed experiments differ from the RAP configuration in notable aspects for obtaining the variable. The microphysics scheme varies between the configurations, also others such as the surface layer and the planetary boundary layer. The wind-shear obtained from the WRF-ARW is sensitivity to variations in these parametrizations (Storm & Basu, 2010; Carvalho *et al.*, 2012). Likewise, aspects that the WRF-ARW and RAP experiments do not share, such as data assimilation and the vertical levels used must be considered.

Figure 12 shows wind roses of LLWS at different heights calculated over “José Martí” International Airport. We compute LLWS from RAP analysis, WSM5 and Lin microphysics, because this schemes showed the better performance in our experiments. Wind roses corresponds to dry season study case, in this period, storms were results of a minor convection intensity, and LLWS was more related to cold front wind discontinuities. In our experiments, to obtained wind at upper levels, we interpolate to a grid with longitudinal resolution of 0.87 km and a latitudinal resolution of 0.5 km, from a 4 km resolution data and we applied a consistent mass model correction. For LLWS from RAP data we interpolate directly to point over airport form 13 km resolution.

Near the aerodrome, there is multiple obstacles with heights comparable to the lower layer altitude. LLWS speed is less intense than RAP forecast at this layer. Also, LLWS direction frequency distribution differs more than other heights. Mass model correction was applied for guarantees the conservation of wind direction due to the impenetrability conditions, this is the probably reason of remarkable differences. For the rest of layers, RAP analysis, WSM5 and Lin scheme depict similar LLWS direction distributions frequencies. Wind roses for rainy season study cases did not show the same homogeneity in distributions, it is consequence of LLWS due to local phenomena. Besides tropical waves imposed a synoptic flux, RAP domain not include the south of western Cuba, and LLWS is more relative to small-scale process, therefore, wind roses depict substantial variations (Figure 13).

CONCLUSIONS

In summary, we developed a microphysics sensitivity study pre-, in-, and, after- storms, to provide the best WRF-ARW model configuration for the forecasting of LLWS derived from storms in "José Martí" International Airport.

The impact of microphysics schemes on temperature, surface pressure, relative humidity, and precipitation has been discussed. The schemes did not show bigger differences among themselves. However, the model did well for temperature, the rest of the variables have superior biases in presence of storms. Precipitation verification shows that the precipitation field should be sensitive to storm features strongly dependent of microphysics schemes. During the dry season, the Lin scheme has the better results

Moreover, LLWS derived from storms sensitivity was evaluated. Microphysics schemes derived dissimilarities winds barbs verticals profiles for weak and deep convection; each hydrometeor particle concentration predicted by tested microphysics has an influence on vertical wind profiles, particularly, for inferior heights. Pearson correlation coefficient between the wind shear speed in the 0-2000 ft layer obtained from the AFWA-diagnostics module and the methodology applied in this investigation was obtained. Once more, Lin scheme has better behavior in the dry season, with a correlation upper than 0.9.

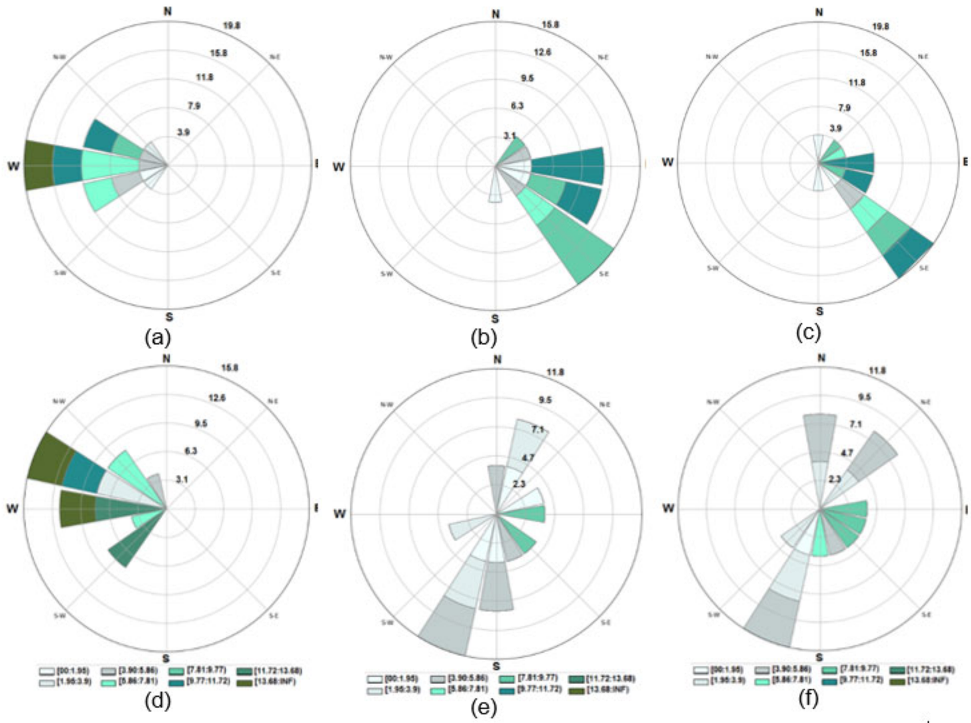

Figure 12. Wind roses for January 27, 2019, panel from left to right RAP, Lin and WSM5 LLWS forecast at (a,b,c) 0-360 ft (d,e,f) 0-1060 ft (g,h,i) 0-1770 ft (j,k,l) 0-2500 ft.

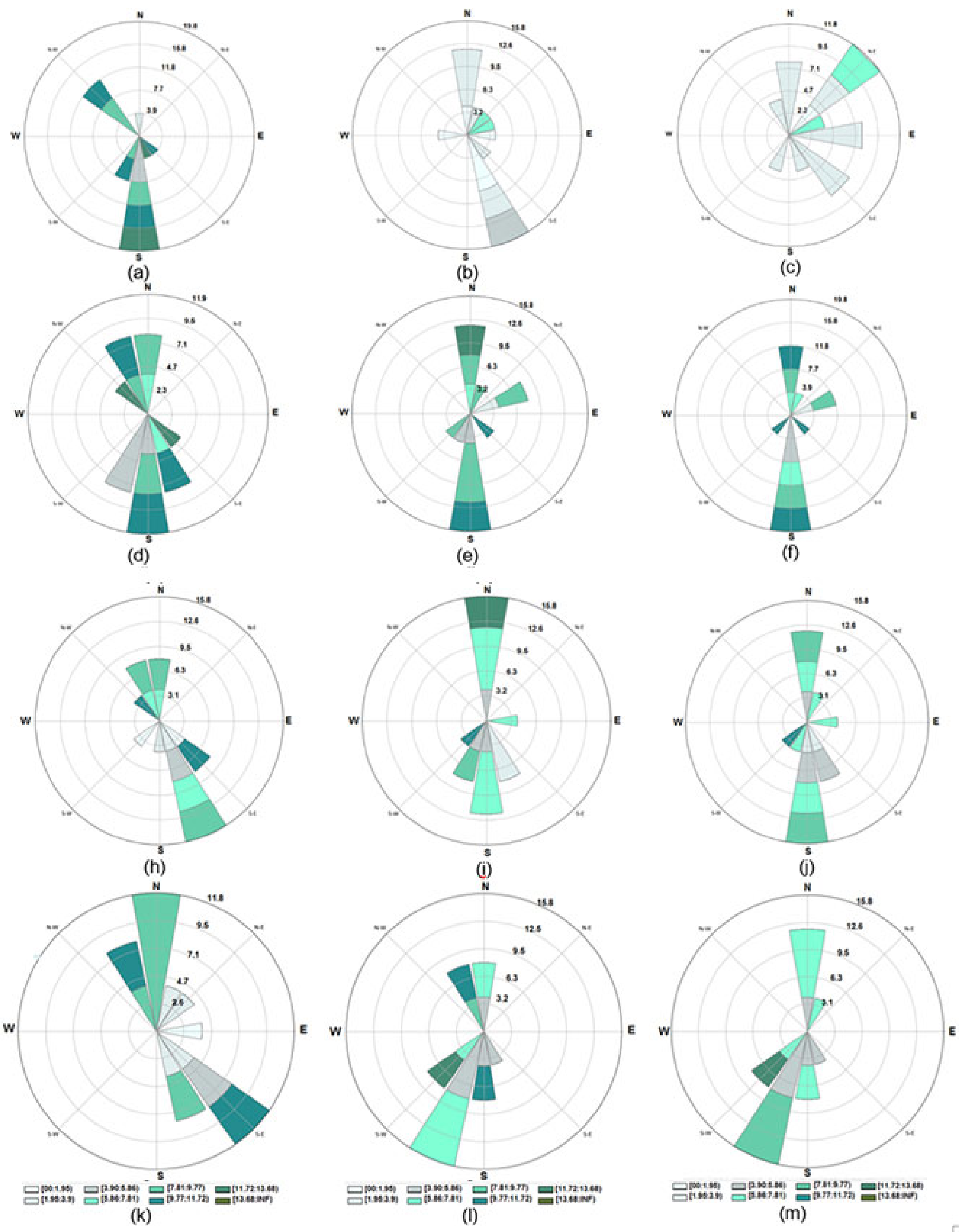

Figure 13. Wind roses for July 3, 2016, panel from left to right RAP, Lin and WSM5 LLWS forecast at (a,b,c) 0-360 ft and (d,e,f) 0-2500 ft.

Furthermore, Taylor diagrams for rainy season LLWS speed forecast pre-, in- and after- storms for different heights levels were computed. Accuracy differences between before-, in- and after- storms LLWS speed forecast are very high when compared to statics among calculation layers. WSM5 and Lin showed the better performance in our experiments. As consequence, wind roses were plotted for LLWS forecast with RAP, WSM5 and Lin configurations. LLWS speed is less intense than RAP forecast at lower levels. This is a probably consequence that near the aerodrome there is multiple obstacles, and in our methodology for WRF-ARW microphysics schemes evaluation mass model correction was applied. Also, considerable variations in distribution frequencies LLWS direction and speed were more relative to small-scale process.

Those results are the first attempt to develop a valuable tool for the improvement of the Aeronautical Meteorological Service of the Cuban Civil Aviation. Ongoing work will therefore include other sensitivity parametrizations analysis.

DATA AVAILABILITY

Observational data were obtained from weather stations placed in the study area maintained by INSMET. Cuban Aeronautical Meteorological Service provided airport meteorological data. The outputs of the WRF-ARW model can be reproduced by performing the simulations with the initialisation data. The outputs of the GFS are freely available at https://nomads.ncep.noaa.gov/cgi-bin/filter_gfs_0p50.pl. On the other hand, radars products were obtained from the Key West, Florida, United States (KBYX) doppler radar (available online at https://www.ncdc.noaa.gov/nexradinv/chooseday.jsp?id=kbyx). Also, the software NOAA Weather and Climate Toolkit v.4.5.0 (free available at https://www.ncdc.noaa.gov/wct/install.php) was utilized to analyse the radar data. Rapid Refresh (RAP) analysis are public at https://www.ncdc.noaa.gov/data-access/model-data/model-datasets/rapid-refresh-rap.

ACKNOWLEDGMENTS

Authors would like to thank NOAA for freely available GFS forecast data and Key West radar data.

REFERENCES

Benjamin, S.G.; Weygandt, S.; Brown, J.M.; Hu, M.; Alexander, C.R.; Smrinova, S.; Olson, J..; James, E.P.; Dowell, D.C.; Grell, G.A.; Lin, H.; Peckham, S.E.; Smith, T.L.; Moninger, W.R.; Kenyon, J.S.; Manikin, G. 2016. "A North American Hourly Assimilation and Model Forecast Cycle: The Rapid Refresh". *Monthly Weather Review,* 144: 1669-1694, ISSN: 1520-0493, DOI:10.1175/MWRD-D-15-02421.

Boadh, R. & Satyanarayana, A.N.V. 2016. "Sensitivity of PBL schemes of the WRF-ARW model in simulating the boundary layer flow parameters for their application to air pollution dispersion modeling over a tropical station". *Atmósfera*, 29(1): 61-81, ISSN: 0187-6236, DOI:10.20937/ATM.2016.29.01.05.

Boilley, A.; Mahouf, J.-F. & Lac, C. 2008. "High resolution numerical modeling of low level windshear over the Nice-Côte d'Azur Airport". In: 13th American Meteorology Society Conference on Mountain Meteorology, Session9A.2, United States of America, pp. 11-15, Available: <https://ams.confex.com/ams/13MontMet17AP/webprogram/Paper141049>, [Consulted: August 22, 2021] .

Campbell, S.D. & Olson, S. 1987. "Recognizing low-altitude wind shear hazards from Doppler weather radar: an artificial intelligence approach". *Journal of Atmospheric and Oceanic Technology,* 4(1): 5-18, ISSN: 0739-0572, DOI: 10.1175/1520-0426(1987)004<0005:RLAWSH>2.0.CO;2.

Carvalho, D.; Rocha, A.; Gómez-Gesteira, M. & Santos, C. 2012. "A sensitivity study of the WRF model in wind simulation for an area high wind energy". *Environmental Modelling & Software*, 33: 23-34, ISSN: 1364-8152, DOI: 10.1016/j.envsoft.2012.01.2019.

Chan, P.W. & Lee, Y.F. 2011. "Application of a groundbased, multi-channel microwave radiometer to the alerting of low-level windshear at an airport". *Meteorologische Zeitschrift*, 20(4): 423-429, ISSN: 0941-2948, DOI: 10.1127/0941-2948/2011/0275.

Chan, P.W. & Lee, Y.F. 2012. "Application of short-range LIDAR in wind shear alerting". *Journal of Atmospheric and Oceanic Technology,* 29(2): 207-220, ISSN: 0739-0572, DOI: 10.1175/JTECH-D-11-00086.

Chan, P.W. & Hon, K.-K. 2016. "Performance of super high resolution numerical weather prediction model in forecasting terrain-disrupted airflow at the Hong Kong International Airport: Case studies". *Meteorological Applications*, 23(1): 101-114, ISSN: 1469-8080, DOI: 10.1002/met.1534.

Coll-Hidalgo, P.; Pérez-Alarcón, A. & González-Jardines, P.M. 2021. "Evaluation of Microphysics Schemes in WRF-ARW Model for Numerical Wind Forecast in José Martí Airport". In: *Proceedings of The 3rd International Electronic Conference on Atmospheric Sciences*. <https://sciforum.net/paper/view/conference/8121> [Consulted: July 15, 2021]

Creighton, G.; Kuchera, E.; Adams-Selin, R.; McCormick, J.; Rentschler, S. & Wickard, B. 2014. "AFWA diagnostics in WRF". <http://www2.mmm.ucar.edu/wrf/users/docs/AFWA-Diagnostics-in-WRF.pdf>. [Consulted: February 12, 2020]

Díaz-Zurita, A.; Góngora-González, C.M.; Lobaina-LaO, A.; Pérez-Alarcón, A. & Coll-Hidalgo, P. 2021. "Numerical mesoscale and short-term wind forecast for the "José Martí" International Airport of Havana". *Revista Brasileira de Meteorologia*, 36(2),171-182, ISSN: 1982-4351, DOI: 10.1590/0102-77863610007.

Dudhia, J. 1989. "Numerical study of convection observed during the winter monsoon experiment using a mesoscale two-dimensional model". *Journal of Atmospheric Sciences*, 46(20): 3077-3107, ISSN: 0022-4928, DOI:10.1175/1520-0469(1989)046<3077:NSOCOD>2.0.CO;2.

García-Diez, M.; Fernández, J.; Fitaand, L. & Yague, C. 2013. "Seasonal dependence of WRF model biases and sensitivity to PBL schemes over Europe". *Quarterly Journal of the Royal Meteorological Society*, 139(671): 501-514, ISSN:1477-870X, DOI:10.1002/qj.1976.

Grell, G.A. & Freitas, S.R. 2013. "A scale and aerosol aware stochastic convective parameterization for weather and air quality modelling". *Atmospheric Chemestry and Physics Discussion*, 13(23): 23845-23893, ISSN: 1680-7316, DOI:10.5194/acp-14-5233-2014.

Han, J.Y.; Baik, J.J. & Khain, A.P. 2012. "A numerical study of urban aerosol impacts on clouds and precipitation". *Journal of Atmospheric*

Sciences, 69(2): 504-520, ISSN: 0022-4928, DOI:10.1007/s13143-014-0016-7.

Halder, M.; Hazra, A.; Mukhopadhyay, P. & Siingh, D. 2015. "Effect of the better representation of the cloud ice-nucleation in WRF microphysics schemes: A case study of a severe storm in India". *Atmospheric Research*, 154: 155-174, ISSN: 0169-8095, DOI:10.5194/angeo-30-897-2012.

Hermes, L.G.; Witt, A. & Smith, S.D. 1993. "The gust-front detection and wind-shift algorithms for the terminal Doppler weather radar system". *Journal of Atmospheric and Oceanic Technology,* 10, 693-709, ISSN: 0739-0572, DOI: 10.1175/1520-0426(1993)010<0693:TGFDAW>2.0.CO;2.

Hon, K.-K. 2018. "Simulated satellite imagery at sub-kilometre resolution by the Hong Kong observatory". *Weather*, 73: 139-144, ISSN: 431656, DOI:10.1002/met.1534.

Hon, K.-K. 2020. "Predicting Low-Level Wind Shear Using 200-m-Resolution NWP at the Hong Kong International Airport". *Journal of Applied Meteorology and Climatology*, 59: 193-207, ISSN: 1558-8424, DOI:10.1175/JAMC-D-19-0186.1.

Hong, S.-Y.; Dudhia, J. & Chen, S.-H. 2004. "A revised approach to ice microphysical processes for the bulk parameterization of clouds and precipitation". *Monthly Weather Review*, 132: 103-120 ISSN: 1520-0493, DOI: 10.1175/1520-0493(2004)132<0103:ARATIM>2.0.CO;2.

Hong, S.-Y & Lim, J.-O.J. 2006. "The WRF single-moment 6-class microphysics scheme (WSM6)". *Journal of the Korean Meteorological Society*, 42: 129-151, ISSN: 1598-3560, DOI: 10.1155/2010/707253.

Hu, X.-M; Nielsen-Gammon, J.W. & Zhang, F. 2012. "Evaluation of three planetary boundary layer schemes in the WRF model". *Journal of Applied Meteorology and Climatology*, 49(9): 1831-1844, ISSN: 1558-8424, DOI: 10.1175/2010JAMC2432.1.

Hu, X.-M.; Klein, P.M. & Xue, M. 2013. "Evaluation of the update YSU planetary boundary layer scheme with in WRF for wind resource and air quality assessments". *Journal of Geophysical Research: Atmospheres*, 118(8): 10490-10505, ISSN: 0148-0227, DOI:10.1002/jgrd.50823.

Iribarne, J.V. & Godson, W.L. 1981. "Atmospheric Thermodynamics". In *Geophysics and Astrophysics Monographs*, 2nd ed.; B.M. McCormac, Ed.; Kluwer Academic Publishers: Boston, MA, USA; pp. 259.

Janjić, Z.I. 2001. "Nonsingular implementation of the Mellor-Yamada level 2.5 scheme in the NCEP Meso Model". *NCEP Office Note 437.*

Lihui, J.; Baiquan, T.; Xinglong, X. ; Zibo, Z. & Bin, Y. 2012. "Numerical simulations of low attitude wind shear based on Doppler lidar. Infrared Laser". *Infrared and Laser Engineering*, 41(7): 1761-1766, ISSN: 1007-2276.

Jolliffe, I. & Stephenson, D. 2003. "Forest Verification: a practitioner's guide in atmospheric science". In: *John Wiley Sons Ltd, The Atrium, Southern Gate,* Chichester, West Sussex PO19 8SQ, England, pp. 37-97.

Lin, Y.-L.; Farley, R.D. & Orville, H.D. 1983. "Bulk parameterization of the snow field in a cloud model". *Journal of Applied Meteorology and Climatology,* 22(6): 1065-1092, ISSN: 1558-8424, DOI:10.1175/1520-0450(1983)022<1065:BPOTSF>2.0.CO;2.

Liu, C. & Moncrieff, M.W. 2007. "Sensitivity of Cloud-Resolving Simulations of Warm-Season Convection to Cloud Microphysics Parameterizations". *Monthly Weather Review*, 135(8): 2854-2868, ISSN: 1520-0493, DOI: 10.1175/MWR3437.1.

Liu, C.; Ikeda, K.; Thompson, G.; Rasmussen, R. & Dudhia, J. 2011. "High-Resolution Simulations of Wintertime Precipitation in the Colorado Headwaters Region: Sensitivity to Physics Parameterizations". *Monthly Weather Review*, 139(11): 3533-53, ISSN: 1520-0493, DOI:10.1175/MWR-D-11-00009.1

Miao, J.F.; Wyser, K.; Chen, D. & Ritchie, H. 2009. "Impacts of boundary layer turbulence and land surface process parameterizations on simulated sea breeze characteristics". *Annales Geophysicae*, 27(6): 2303-2320, ISSN: 1432-0576, DOI:10.5194/angeo-27-2303-2009.

Mlawer, E.J.; Taubman, S.J.; Brown, P.D.; Iacono, M.J. & Clough, S.A. 1997. "Radiative transfer for inhomogeneous atmospheres: RRTM, a validated correlated-k model for the longwave". *Journal of Geophysical Research: Atmospheres*, 102(D14): 16663-16682, ISSN: 0148-0227, DOI: 10.1029/97JD00237.

Montero, G.; Montenegro, R.; Escobar, J.; Rodríguez, E. & González, J. 2006. "Modelización y simulación numérica de campos de vientos orientados a procesos de contaminación atmosférica". Instituto Universitario de Sistemas Inteligentes y Aplicaciones numéricas en Ingeniería, Universidad de Las Palmas, Gran Canaria <http://www-lacan.upc.es/projects/CLI, Modelización Numéricas de Problemas Medioambientales de Convección-Difusión-Reacción> [Consulted: August 21, 2021]

Morrison, H.; Thompson, G. & Tatarskii, V. 2009. "Impact of cloud microphysics on the development of trailing stratiform precipitation in a simulated squall line: Comparison of one- and two-moment schemes". *Monthly Weather Review*, 137(3): 991-1007, ISSN: 1520-0493, DOI: 10.1175/2008MWR2556.1.

OACI. 2005. "Manual on Low-Level Wind Shear". *Doc 9817 AN/449*, pp. 1-8 <https://standards.globalspec.com/std/471313/9817> [Consulted: March 10, 2021]

Otkin, J.A. & Greenwald, T.J. 2008. "Comparison of WRF Model-Simulated and MODIS-Derived Cloud Data". *Monthly Weather Review*, 136(6): 1957-70, ISSN: 1520-0493, DOI: 10.1175/2007MWR2293.1.

Pérez-Bello, A.; Mitrani, A.I.; Díaz, R.O.; Wettre, C. & Robert, L. H. 2019. "A numerical prediction system combining ocean, waves and atmosphere models in the Inter-American Seas and Cuba". *Revista Cubana de Meteorología*, 25(1): 109-120, ISSN: 2664-0880 <http://rcm.insmet.cu/index.php/rcm/article/view/459> [Consulted: January 15, 2021]

Rajeevan, M.; Kesarkar, A.; Thampi, S.; Rao, T.; Radhakrishna, B. & Rajasekhar, M. 2010. "Sensitivity of WRF cloud microphysics to simulations of a severe thunderstorm event over southeast India". *Annales Geophysicae*, 28(2): 603-619, ISSN: 1432-0576, DOI: 10.5194/angeo-28-603-2010.

Reisner, J.; Rasmussen, R.M. & Bruintjes, R.T. 1998. "Explicit forecasting of supercooled liquid water in winter storms using the MM5 mesoscale model". *Quarterly Journal of the Royal Meteorological Society*, 124(548): 1071-107, ISSN: 1477-870X, DOI:10.1002/qj.49712454804

Sánchez, E.O. 2018. Evaluation of the medium-term forecast of the atmospheric component of the SPNOA with data from INSMET meteorological stations. *Bachelor Thesis*, Higher Institute of Technologies and Applied Sciences, Havana, Cuba, 2018.

Sari, F.P.; Baskoro, A.P. & Hakim, O.S. 2018. "Effect of different microphysics scheme on WRF model: A simulation of hail event study case in Surabaya, Indonesia". In: *Proceedings of the American Institute of Physics Conference,* 1987(1), 020002, DOI:10.1063/1.5047287.

Shaw, B.; Spencer, P.; Carpenter, J. & Barrere, J. 2008. "Implementation of the WRF model for the Dubai International Airport aviation weather decision support system". In: *Proceedings of the 13 th Conference on Aviation, Range and Aerospace Meteorology*, New Orleans, United States of America, 5.2. <https://ams.confex.com/ams/88Annual/techprogram/paper_133147.html> [Consulted: January 10, 2021]

Shrestha, R.K.; Connolly, P.J. & Gallagher, M.W. 2017. "Sensitivity of WRF Cloud Microphysics to Simulations of a Convective Storm Over the Nepal Himalayas". *The Open Atmospheric Science Journal*, 11(1): 29-43, ISSN: 1874-2823, DOI: 10.2174/1874282301711010029.

Shun, C. M. & Chan, P. W. 2008. "Applications of an infrared Doppler LIDAR in detection of wind shear". *Journal of Atmospheric and Oceanic Technology*, 25(5), 637-655, ISSN: 0739-0572, DOI: 10.1175/2007JTECHA1057.1.

Sierra, L.M.; Ferrer, H.A.L.; Valdés, R.; Mayor, Y.; Cruz, R.; Montejo, I.; Rodríguez, C.F.; Rodríguez, N.; Roque, A. 2015. "Automatic mesoscale prediction system of four daily cycles". Technical Scientific Report. DOI: 10.13140/RG.2.1.2888.1127

Sierra, M.; Borrajero, L.; Ferrer, A.L.; Morfa, Y.; Yordanis, A.; Loyola, M. & Hinojosa, M. 2017. "Sensitivity studies of the SisPI to changes in the PBL, the number of vertical levels and the microphysics and clusters parameterizations, at very high resolution". Technical Scientific Report. DOI: 10.13140/RG.2.2.29136.00005.

Skamarock, W.C.; Klemp, J.B.; Dudhia, J.; Gill, D.O.; Barker, D.M.; Wang, W. & Power, J.G. 2005. "A description of the advanced research WRF version 2". *NCAR Tech Note NCAR/TN 468 STR*, National Center for Atmosferic Research, Boulder, Colo.

Skamarock, W.C.; Klemp, J.B.; Dudhia, J.; Gill, D.O.; Barker, D.M.; Wang, W. & Power, J.G. 2008. "Description of the Advanced Research WRF Version 3". *NCAR Tech Note NCAR/TN 475 STR*, UCAR Communications, Boulder, Colo.

Somos-Valenzuela, M. & Manquehual-Cheuque, F. 2020. "Evaluating Multiple WRF Configurations and Forcing over the Northern Patagonian Icecap (NPI) and Baker River Basin". *Atmósfera*, 11(815), 19, ISSN: 0187-6236, DOI: 10.3390/atmos11080815.

Sosa, A. 2018. "International Airport "José Martí" low-level wind shear characteristics during 2012-2017 period". *Bachelor Thesis*, Higher Institute of Technologies and Applied Sciences, Havana, Cuba.

Srikanth, M.; Satyanarayana, A.N.V. & Rao, T.N. 2014. "Performance evaluation of PBL and cumulus parameterization schemes of WRF ARW model in simulating severe thunderstorm events over Gadanki MST radar facility. -Case study". *Atmospheric Research*, 139: 1-17, ISSN: 0169-8095, DOI: 10.1016/j.atmosres.2013.12.017.

Srinivas, C.V.; Venkatesan, R. & Bagavath Singh, A. 2007. "Sensitivity of mesoscale simulations of land-sea breeze to boundary layer turbulence parameterization". *Atmospheric Environment*, 41(12): 2534-2548, ISSN: 1352-2310, DOI: 10.1016/j.atmosenv.2006.11.027.

Storm, B. & Basu, S. 2010. "The WRF Model Forecast-Derived low-level wind shear climatology over the United States Great Plains". *Energies*, 3, 258-276, ISSN: 1996-1073, DOI: 10.3390/en3020258.

Tewari, M.; Chen, F.; Wang, W.; Dudhia, J.; LeMone, M.A.; Mitchell, K.; Ek, M.; Gayno, G.; Weigel, J. & Cuenca, R.H. 2004. "Implementation and verification of the unified NOAH land surface model in the WRF model". In: *Proceedings of the 20th Conference on Weather Analysis and Forecasting/16th Conference on Numerical Weather Prediction*, Seattle, WA, USA; 17.5, pp. 11-15.

Urlea, A.-D. & Pietrisi, M. 2015. "Study of the Low Level Wind Shear using AMDAR reports". *EGU General Assembly Conference Abstracts,* pp. 2185, <https://ui.adsabs.harvard.edu/abs/2015EGUGA..17.2185U> [Consulted: August 21, 2021]

Wilson, W.; Roberts, R.D.; Kessinger, C. & McCarthy, J. 1984. "Microburst wind structure and evaluation of Doppler radar for airport wind shear detection". *Journal of Applied Meteorology and Climatology*, 23(6), 898-915, ISSN: 1558-8424, DOI: 10.1175/1520-0450(1984)023<0898:MWSAEO>2.0.CO;2.

Conflicts of Interest: The authors declare that there is no conflict of interest regarding the publication of this paper.

Authors Contributions: Conceptualization: P.C.-H., C.M.G-G. and P.M.G.-J. **Methodology**: P.C.-H. **Software**: P.C.-H.; A.P.-A. and P.M.G.-J. **Validation**: P.C.-H. **Formal Analysis**: P.C.-H. Investigation: P.C.-H. and A.P.-A. **Data curation**: P.C.-H., A.D-Z and P.M.G.-J. **Writing-original draft preparation**: P.C.-H. **Writing-review and editing**: P.C.-H., A.D-Z and A.P.-A. **Visualization**: P.C.-H. and A.P.-A. **Supervision**: A.P.-A., C.M.G-G. and P.M.G.-J. **All authors have read and agreed to the published version of the manuscript.**